Available online at www.sciencedirect.com
SCIENCE DIRECT
Journal of Photochemistry and Photobiology A: Chemistry 181 (2006) 385–393
Journal of Photochemistry and Photobiology A:Chemistry
www.elsevier.com/locate/jphotochem

Using silica films and powders modified with benzophenone to photoreduce silver nanoparticles

Susie Eustis [b], Galina Krylova [a], Natalie Smirnova [a], Anna Eremenko [a,*], Christopher Tabor [b], Wenyu Huang [b], Mostafa A. El-Sayed [b,*]

[a] *Institute of Surface Chemistry, National Academy of Sciences, General Naumov str., 17, 03164 Kyiv, Ukraine*
[b] *Laser Dynamics Laboratory, School of Chemistry and Biochemistry, Georgia Institute of Technology, Atlanta, GA 30332, United States*

Received 15 February 2005; received in revised form 16 December 2005; accepted 19 December 2005
Available online 7 February 2006

Abstract

Porous silica (SiO_2 films and powders), modified with benzophenone (BP), facilitates the formation of stable sliver nanoparticles by taking advantage of the solid supported photosensitizer. The silica serves as a carrier for the BP into an aqueous solution and its subsequent removal. Benzophenone, bound to a silica film, was able to reduce silver ions to generate nanoparticles in solution, while silica powder with bound BP generates silver nanoparticles that are attracted to the silica. Silver nanoparticles are also fabricated in porous silica films by incorporating silver ions into the films before casting and then irradiating the film in a solution containing BP. From pH studies, it is concluded that the ketyl-radicals and anion-radicals of BP and IPA both take part in the reduction of silver ions. These synthetic studies provide a new photochemical reduction method by immobilizing the reactant on a silica surface allowing generation of silver nanoparticles in solution attached to powders or inside a film for catalytic applications or increased conductivity of silica films.

Keywords: Mesoporous silica films; Silver nanoparticles (Ag NP); Benzophenone (BP); Ketyl-radicals; Photoreduction; Surface plasmon resonance (SPR)

1. Introduction

Modification of silica surfaces with photoactive organic compounds generates heterogeneous photosensitive materials that can be used in light conversion systems, in non-linear optics, or as reducing agents. In addition, these modified silica surfaces could be useful for catalysis and the removal of noble and toxic transition metal ions from solutions; accordingly, it is beneficial to have a large surface area for the photocatalyst and other species to bind. The well known photochemical reaction of benzophenone (BP) with isopropyl alcohol [1–4] can be carried out at the silica interface by immobilizing BP on the surface, which produces a material with a high photoreductive yield that is capable of removing transition and noble metal ions from aqueous solution. Metal nanoparticles have attracted considerable attention due to their interesting optical properties such as large non-linear sensibility, surface enhanced Raman scattering, and their use in photophysics [5] and photochemistry [6]. Furthermore, SiO_2-BP systems could become competitive with the widely used photocatalyst TiO_2. Initial research into reducing silver on SiO_2 surfaces has previously been presented by various researchers [7–12].

In this work, the photo sensitizer benzophenone was adsorbed onto the surface of photochemically inactive silica. Mesoporous silica films were synthesized via the low-temperature sol–gel process consisting of the acid hydrolysis of tetraethoxysilane in the presence of template agents. Commercially available porous silica powders were also used. The activity of SiO_2-BP films and powders as photoreducing agents to generate silver nanoparticles was studied as a function of the substrate structure and BP concentration.

2. Materials and methods

2.1. Reagents

The following chemicals were used as received: Silica gel (SiO_2) powders (SG-150 Å Davisil) with specific surface area of

* Corresponding authors.
E-mail addresses: annaerem@voliacable.com (A. Eremenko), mostafa.el-sayed@chemistry.gatech.edu (M.A. El-Sayed).

1010-6030/$ – see front matter © 2006 Elsevier B.V. All rights reserved.
doi:10.1016/j.jphotochem.2005.12.024

300 m^2/g (Aldrich), colloidal silica Du Pont Ludox AM-30 with surface areas from 210 to 230 m^2/g (Aldrich), $AgNO_3$, sodium dodecylsulphate (SDS, Aldrich), Pluronic $EO_{20}PO_{70}EO_{20}$ (P123, Aldrich), ethanol (Fluka), and tetraethoxysilane 98% (TEOS, Aldrich).

Benzophenone (BP, Fluka) was purified by double recrystallization from ethanol. Isopropyl alcohol (IPA) (Fluka) and hexane (Fluka) were purified by repeated distillation.

2.2. Silica film preparation

The mesoporous silica films were prepared by the sol–gel method using a template, non-ionic, tri-block copolymer Pluronic (P123) as described in the literature [13–15]. The precursor sol was prepared by hydrolysis of TEOS in a mixture of distilled water, ethanol, and 1 M HNO_3 solution. After 24 h of prolonged hydrolysis, a solution of P123 in ethanol was added. The total molar ratio of the precursor was 1 TEOS:0.008 P123:0.16 HNO_3:15 H_2O:15 C_2H_5OH. The coatings were deposited onto clean glass substrates by the dip-coating technique. The films were dried for 12 h at ambient temperature, followed by heat treatment at 400° C with a rate of 1° C/min and held at 400° C for 6 h.

2.3. Generation of BP coated SiO_2 films and powders

Silica gel powders (purchased) and films (described above in Section 2.2) were thermally pretreated at 250° C. To measure the adsorption isotherm of BP on the silica surface, the SiO_2 films and powders were placed in a BP–hexane solution with a BP initial concentration in the range of 10^{-5} to 10^{-3} M for 24 h until the adsorption remained constant. The amount of adsorbed BP molecules was monitored by measuring the decrease in the optical density of the remaining BP–hexane solution at 355 nm.

2.4. Photoreduction solutions containing BP in aqueous solution

Conditions are identical to those reported previously [16]. Briefly, $AgNO_3$, BP, Ludox (colloidal silica), and IPA are present in aqueous solution. No additional silica is present in this solution.

2.5. Photoreduction solutions containing SiO_2-BP films and powders

The porous silica (SiO_2-BP) powders and films, after BP adsorption (as described in Section 2.3), were used as a removable photoreducing agent. The reaction mixture consisted of a 40 ml aqueous solution of 1.5×10^{-4} M $AgNO_3$, 0.4 M IPA, and 1% Ludox. SiO_2-BP films and 0.5 g of SiO_2-BP powder were placed into separate solutions and vigorously stirred for 10 min before irradiation to establish desorption/adsorption equilibrium of BP from the film or powder with the solution. Ludox, colloid silica stabilized with tetramethylhydroxylamine, also acted as a stabilizer in this system.

2.6. Generation of SiO_2-Ag films

SiO_2-Ag films were prepared with a 0.1 Ag/SiO_2 molecular ratio. An aqueous solution of $AgNO_3$ was added to hydrolyzed silica sol before film deposition. After calcinations in air at 400° C, transparent colorless films were produced with no traces of silver nanoparticles. Irradiation of the SiO_2-Ag film was carried out in an aqueous solution of 1.4×10^{-3} M BP, 1.7×10^{-3} M SDS, and 1.84 M IPA. SDS was used to increase the solubilization of BP in the alcohol–water solution. SDS could also act as a hydrogen donor in the reaction with the BP triplet.

2.7. Irradiation conditions

A monochromatic 1000-W low-pressure mercury lamp connected with a standard cobalt(II) sulfate solution filter was used as a 253.7 nm irradiation source. A 500-W low-pressure mercury lamp combined with the appropriate UV 7-60 filter was used as a source of 365 nm light. A cylindrical quartz vessel with a volume of 40 ml was used as the reaction cell. The incident photon intensity (as determined by a tris(oxalato)ferrate(III) actinometer [17]) was determined at 253.7 and 365 nm to be 2×10^{17} and 2.12×10^{15} cm^{-2} s^{-1}, respectively. Irradiation was carried out while bubbling argon through the solution at room temperature. The absorption spectra of the solutions before and after irradiation were measured with a Lambda UV–vis spectrophotometer (Perkin-Elmer) in a rectangular 1 cm thick quartz cuvette. Diffuse reflectance spectra of SiO_2-BP films and powders were also measured with this spectrophotometer.

2.8. Emission of SiO_2-BP powders

A sample of SiO_2-BP powder ($C_{BP} = 2 \times 10^{-4}$ mol/g) was vacuum-evacuated to a pressure of 1.33×10^{-2} Pa for 1 h in a quartz cell prior to emission measurements. Stationary luminescence spectra were measured on an Analytical Edinburgh Instruments spectrometer with a FS 900CDT steady-state T-geometry Fluorometer, FL 900 CDT.

2.9. Structural investigation instrumentation

X-ray diffraction (XDR, Cu Kα radiation) analysis was performed on the SiO_2 and SiO_2-Ag films using a diffractometer DRON-3 with a minimum glancing angle of $\theta = 0.5$. TEM samples of silver nanoparticle solutions were prepared by spotting a drop of solution onto a carbon-coated copper TEM grid (Ted Pella) and allowing them to dry overnight. They were imaged using an accelerating voltage of 100 kV on a JOEL JEM-100C transmission electron microscope (TEM). A scanning electron microscope (SEM) (LEO 1530) was used to probe the SiO_2-Ag film.

2.10. Aging kinetics after irradiation

To determine the stabilizing effect of BP on silver nanoparticles, the absorbance was measured after irradiation ceased for solutions irradiated with SiO_2-BP film and without. Solutions

were irradiated with 254 nm light for 30 min and stored in the dark for a variable amount of time. The solutions were the same as described in Section 2.5. The SiO_2-BP film was removed from solution immediately after irradiation.

2.11. Conditions for pH measurements

Solutions containing SiO_2-BP powders were used to study the pH kinetics. The aqueous solution contained 1.5×10^{-4} M $AgNO_3$, 0.4 M IPA, 1% Ludox, and 0.5 g of SiO_2-BP powder, where the BP coverage of silica is 1×10^{-4} M BP/g SiO_2 powder. The pH of the starting solution was 7.8. Nitric acid was added to obtain the desired acidic pH. A buffer solution of 0.01 M $Na_2B_4O_7 \cdot 10H_2O$ was added to maintain pH 8.

3. Results and discussion

3.1. Adsorption and desorption of BP from silica surfaces

The adsorption isotherm of BP deposition onto silica in a hexane solution (as described in Section 2.3) is a Langmuir's type curve, which indicates physical adsorption onto the surface. Fig. 1a shows the diffuse reflectance spectrum of SiO_2-BP powder, confirming the presence of BP on the surface. Fig. 1b is the conversion of the diffuse reflectance spectrum to the absorption spectrum using the Shuster–Kubelka–Munk equation [18] showing the two absorption bands of BP. The absorption peaks at 345 and 260 nm correspond to the $n\pi^*$ transition and the $\pi\pi^*$ transition, respectively [19–21].

To investigate the optimum coverage of BP on the silica surfaces (both SiO_2-BP films and powders), the percentage of BP desorbed when washed with a solvent was determined as a function of the initial BP coverage. When the amount of adsorbed BP molecules on SiO_2-BP powder is 8.4% of a monolayer, less than 7% of the adsorbed BP is desorbed when rinsed with hexane. When BP molecules occupied more then 10% of a monolayer, the percent of desorbed molecules after washing sharply increased (supplementary Fig. S.1). This suggests that the silica surface holds BP adsorbed molecules more tightly at 8.4% of a monolayer due to the amount of space necessary for the strong interaction of the benzophenone C=O groups with the ≡Si–OH groups of the silica surface. In the following experiments SiO_2-BP samples are used with adsorbed BP molecules forming ~8% of a monolayer.

To determine the actual amount of BP dissolved into our reaction solutions we measured the absorbance of the BP in solution at various times. Only 0.55% of the adsorbed BP is transferred from the SiO_2-BP powders to the aqueous solution in the first 5 min of contact. After 2 h, this amount slightly increased to 0.64%, equating to a BP concentration of 9.5×10^{-6} M, more than 15 times less than the concentration of Ag^+ in the reaction mixture (supplementary Fig. S.2). The amount of BP desorbed from SiO_2-BP films was lower than our detectable concentration (2.1×10^{-7} M or 0.88% of a monolayer). Thus, the BP triplet is effectively quenched in solution by silver ions [2], and the following experiments present a photoreduction by BP molecules adsorbed on the SiO_2 surface.

In the case when BP and Ag^+ ions are dissolved and irradiated together in solution, as considered in our previous publication [16] (Section 2.4); BP is consumed in the process. In accordance with Demeter and Berces [22], in this case benzpinacol or the long-lived intermediates, generally called "light-absorbing transients" (LAT), are formed by the coupling of a diphenylketyl with a dimethylketyl-radical. To probe for the presence of LATs, a solution of BP in IPA was irradiated to produce LATs. Then, after irradiation was stopped, silver ions were added to the BP–IPA–LAT solution. Immediately after mixing, the characteristic surface plasmon absorption band of silver nanoparticles appeared. Thus silver nanoparticles were created due to the presence of LATs in solution because they are unstable and generate free radicals in the dark. When SiO_2-BP films or powders were used, as presented herein, no surface plasmon absorption band of the silver nanoparticles was observed. These results confirm that minimal concentrations of LATs and BP were present in solution when BP is attached to a silica surface.

3.2. Luminescence spectra of BP on silica powder

Publications of the absorption spectra of BP and luminescence properties of adsorbed BP on silica are few. Turro et al. [23] reported that the triplet energy transfer occurs on the silica surface from adsorbed $^3BP^*$ to naphthalene from diffuse reflectance transient absorption spectroscopy. Thomas [24] pointed to similarities of the spectroscopy and kinetics between

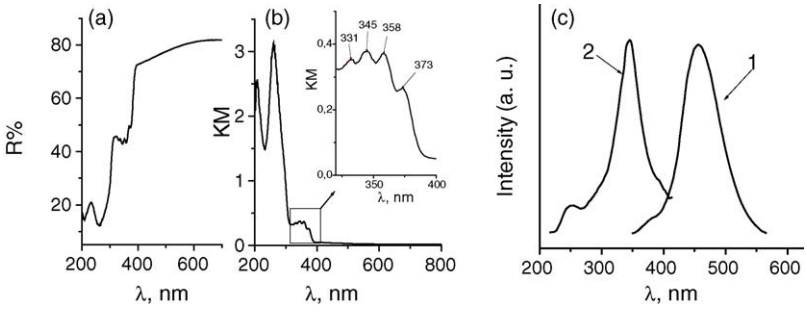

Fig. 1. (a) Diffuse reflectance spectrum of SiO_2-BP powder; (b) absorption spectrum of SiO_2-BP powder from Shuster–Kubelka–Munk conversion, (inset) fine structure of absorption spectrum of SiO_2-BP; (c) emission spectrum of SiO_2-BP powder with 340 nm excitation (1) and excitation spectrum monitored at 460 nm (2).

$^3BP^*$ in a solution of cyclohexane and on a silica surface. The fluorescence of BP in solution has a low quantum yield (10^{-6}) with a very short lifetime of 10^{-11} s [25]. This is due to rapid S_1–T interconversion of the excited singlet state of BP to the biradical highly reactive triplet state. A BP molecule in the T-excited state abstracts a hydrogen atom from aliphatic alcohols to form two ketyl-radicals [3,26].

The emission spectrum of SiO_2-BP powders (as described in Section 2.8) consists of a strong emission at 460 nm with its corresponding excitation peak at 340 nm (Fig. 1c). This emission allows characterization of our material and further confirms the presence of BP on the silica surface. The emission can be assigned to the phosphorescence of adsorbed BP via hydrogen-bonding with OH groups on the silica surface. Nishiguchi et al. [27] analyzed the phosphorescence of BP within zeolites and attributed the emission peak at 465 nm with its excitation at 320 nm to the protonated form of adsorbed BP. Okamoto et al. [28] ascribed the phosphorescence emission of BP adsorbed on silica at 430 nm and its excitation at 330 nm to the hydrogen-bonding of BP to the surface OH groups. The acidity of OH groups on the silica surface is low in comparison with the zeolite surface. We suggest that not all of the OH groups on the silica surface are equal, and a mixture of the strongly and weakly hydrogen-bonded forms of BP is absorbed on the silica powders under vacuum (as used for emission measurements). This is supported by molecular luminescence of an adsorbed dye on a silica surface [29]. In the photoreduction experiment presented in the following sections, adsorbed BP is in contact with solution, thus IPA and water molecules should be partially adsorbed on the silica along with the BP, resulting in a more homogeneous distribution of the strength of the hydrogen-bonded BP on the silica surface.

3.3. Low angle XRD characterization

The porous structure of the silica films synthesized in the presence of various templates was analyzed by low angle XRD measurements. The XRD pattern of the silica film using P123 as a template has a single sharp peak with a maximum at $2\theta = 0.56$ (supplementary Fig. S.3) and can be indexed as a (1 0 0) reflection of hexagonal pore structure [15]. The intensity of the (1 0 0) peak reflects a *d*-spacing of 15.77 nm corresponding to a large unit cell parameter ($a = 2 \times d_{100}/\sqrt{3} = 18.56$ nm). This indicates a mesoporous silica film.

3.4. Using SiO_2-BP films to photoreduce silver ions

The photochemical reduction of silver ions via SiO_2-BP porous films was investigated in a water–alcohol solution (described in Section 2.5) with incident irradiation at 254 and 365 nm from a mercury lamp (Section 2.7). The SiO_2-BP film was immediately removed after irradiation and the absorption spectra of the irradiated solutions were measured. The absorption spectra of reduced silver particles as a function of irradiation time (254 nm) in the presence of a SiO_2-BP film are shown in Fig. 2a. A broad absorption band from the silver nanoparticles (maximum at 407 nm) appeared while in the presence of the stabilizer, Ludox. This absorption is due to the collective surface oscillations of the electrons in metal particles. This absorption occurs when the particle sizes are smaller than the electron mean free path (52 nm for silver [30]). This phenomenon is called a surface plasmon resonance (SPR). The absorption spectra associated with small (3–20 nm) spherical metal nanoparticles obeys Bugger–Lambert–Beer's law, $I = I_0 \exp(-\alpha l C)$, where I_0 and I are the intensities of the incident and transmitted light, respectively, α the absorption coefficient in $1\,mol^{-1}\,cm^{-1}$, l the sample path length in cm, and C is the concentration of metal atoms in $mol\,l^{-1}$. The absorption coefficient of a colloid nanoparticle solution, α, can be defined by the electrostatic equation:

$$\alpha = \frac{18\pi}{\ln 10}\frac{M}{\lambda\rho}\frac{\varepsilon_0^{3/2}\varepsilon'}{(\varepsilon' + 2\varepsilon_0)^2 + (\varepsilon'')^2} \quad (1)$$

where λ is the wavelength; M and ρ the molecular weight and density of a colloidal metal, respectively; ε' and ε'' the real and the imaginary part of the complex dielectric constant of the metal, and ε_0 is the dielectric constant of the surrounding medium. According to Mie theory, the SPR band maximum position is defined by the free electron density on the nanoparticle and the dielectric properties of the metal and solvent [30,31]:

$$\lambda_{max}^2 = \frac{(2\pi c)^2 m_e(\varepsilon_0 + 2n_0^2)}{4\pi e^2 N_e} \quad (2)$$

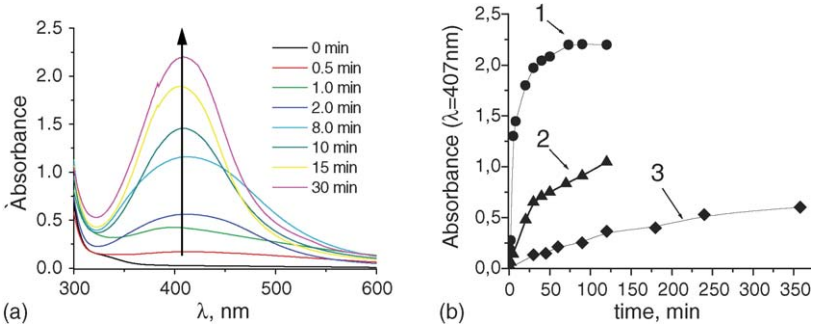

Fig. 2. (a) Absorption spectra of silver nanoparticles generated using SiO_2-BP film at various irradiation times and (b) kinetics of silver nanoparticle formation (measured by the absorbance intensity as a function of irradiation time) using 254 nm irradiation and SiO_2-BP film (●, 1), 254 nm irradiation without SiO_2-BP film (▲, 2), 365 nm irradiation with SiO_2-BP film (♦, 3).

where c is the velocity of light in a vacuum, m_e and e the electron's mass and charge, respectively, ε_0 the high-frequency dielectric constant of the metal, n_0 the refractive index of the solvent, and N_e is the free electron density on the metal nanoparticles. The theoretical absorption maximum of the SPR band for silver nanoparticles in air is located at 360 nm, in water at 390 nm, and in glass at 410 nm [5]. The surface plasmon in this experiment was observed between 403 and 407 nm [32]. Using the effective medium model one can obtain $n_0 = 1.43$ to match our observed surface plasmon maximum, which is a value between water ($n_0 = 1.33$) and amorphous SiO_2 ($n_0 = 1.54$).

The intensity of the SPR absorption band at 407 nm is proportional to the nanoparticle concentration and is plotted versus irradiation time in Fig. 2b. Photoreduction with $\lambda = 253.7$ nm was more effective in the presence of the SiO_2-BP film than in the absence of the silica film (Fig. 2b). Irradiation with 365 nm light decreases the photoreduction rate by almost two orders of magnitude compared with 253.7 nm. However, this is because the intensity of the 365 nm light source is two orders of magnitude weaker than the 253.7 nm light. Thus, the presence of SiO_2-BP films is able to increase the rate and yield of nanoparticles generated for both 253.7 and 365 nm light.

To quantitatively calculate the quantum yields with SiO_2-BP films, we have linearly fit the absorption maximum observed in Fig. 2b at early times. The slope, k, is proportional to the constant of the quasi-zero order reaction rate or the change of absorbance (ΔA) during irradiation time Δt ($k = \Delta A/\Delta t$). The quantum yield is expressed as $\Phi = (\Delta N/\Delta t)/n$, where ΔN is an amount of silver ions reduced in time Δt, and n is the number of absorbed photons (estimated by actinometry) [33]. The amount of reduced silver nanoparticles can be determined from the absorption of the solution $\Delta N = \Delta A V N_A/\alpha l$, where V is the volume of irradiated solution, N_A Avogadro's number, α the absorption coefficient of Ag NP solution, and l is the cuvette thickness. Thus, replacing ΔN for the quantum yield generates the equation $\Phi = kVN_A/\alpha l n$. The value of the absorption coefficient of silver nanoparticles used in the quantum yield calculation ($\alpha = 1.46 \times 10^4\ M^{-1}\ cm^{-1}$) was estimated from experimental data, by dividing the final absorbance at 407 nm by the initial Ag^+ concentration (1.5×10^{-4} M), and it is in agreement with Henglein [34] where $\alpha = 1.5 \times 10^4\ M^{-1}\ cm^{-1}$ for small silver nanoparticles. The value of α calculated from Eq. (1) is $1.7 \times 10^4\ M^{-1}\ cm^{-1}$.

Similar photoreduction quantum yields were calculated for both irradiation wavelengths using SiO_2-BP films, namely 2.73% and 2.65% for 253.7 and 365 nm irradiation, respectively. The conditions of the blank experiment were similar to that of Hada et al. [35]. The quantum yield for the blank irradiation was 0.3%, about nine times less than in the presence of the SiO_2-BP film. In the absence of SiO_2-BP film, silver nanoparticle formation was not observed with 365 nm irradiation. Thus, the SiO_2-BP films were solely responsible for the observed generation of silver nanoparticles in this study. Other background studies with only BP in solution have already been performed [2,3]. Silica film alone is not photoactive and cannot contribute to the photoreduction process [9]; therefore its presence in solution would lead to similar results as those preformed in water [35].

3.5. Aging kinetics after irradiation of silver nanoparticles with SiO_2-BP films

Silver nanoparticles were unstable in solution and were observed to precipitate after irradiation had ceased (Section 2.10). This was indicated by the decrease in the SPR absorbance spectra in Fig. 3a. No shifting of the SPR absorption peak occurred, which is characteristic of nanoparticle aggregation [36,37]. When SiO_2-BP films were used in the reduction of silver, a slower absorption decrease was observed compared to the blank experiment (water–IPA solution without SiO_2-BP) (Fig. 3a and b).

The peptizing action of BP ketyl-radicals could have been responsible for the apparent stabilization of Ag colloids [23,25,38]:

$$(C_6H_5)_2C^{\bullet}OH + (Ag^0)_n \rightarrow (C_6H_5)_2CO + (Ag^0)_n{}^- + H^+$$

Perhaps due to peptization in the presence of SiO_2-BP films, the silver nanoparticles were more negatively charged than in the blank experiment, thus enhancing their stability. Fig. 4 presents the TEM image of silver nanoparticles formed in solution with Ludox particles (as described in Section 2.4). The attraction of the Ludox and silver nanoparticles is attributed to stronger

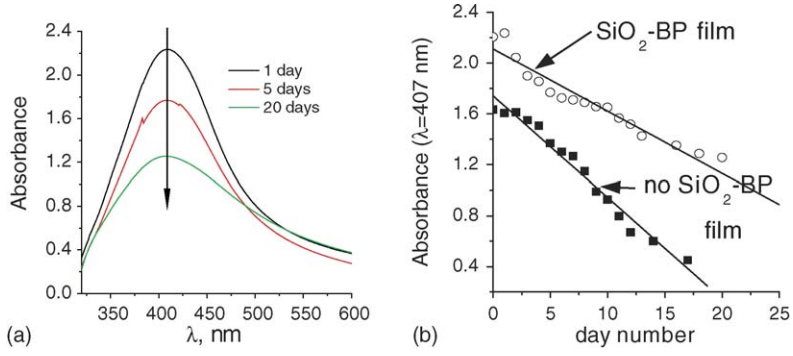

Fig. 3. (a) Absorption spectra of silver nanoparticles generated using SiO_2-BP film after 30 min of irradiation stored in the dark for the indicated time and (b) kinetics of silver nanoparticle SPR absorption at 407 nm generated with SiO_2-BP film (◯) and without SiO_2-BP film (■).

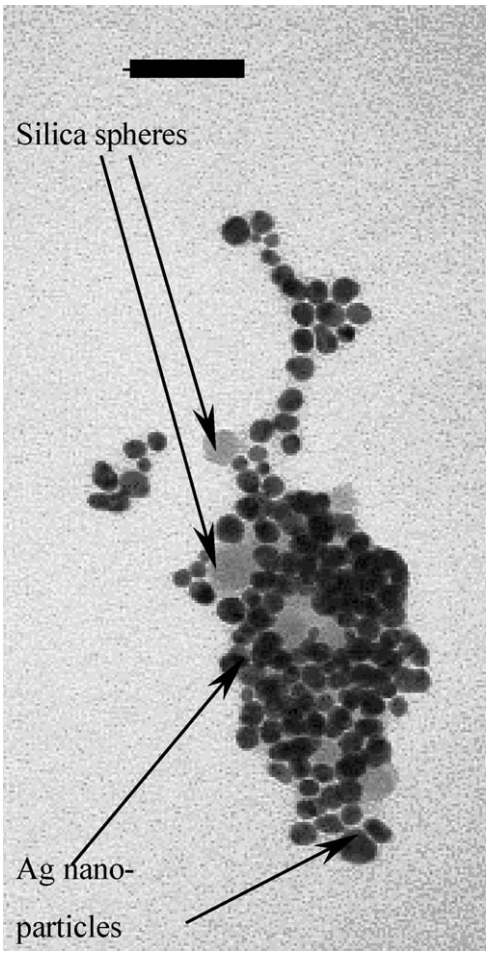

Fig. 4. TEM image of silver nanoparticles generated with BP-solution and Ludox (silica particles). Scale bar is 50 nm.

interaction forces between these two materials than between two silver particles.

3.6. Reduction of silver with SiO_2-BP powders

Solutions of silver nanoparticles generated with SiO_2-BP powder (Section 2.5) had the largest decrease in the surface plasmon resonance absorption after irradiation (Section 2.7) due to deposition of the silver particles onto the SiO_2-BP powder surface. Diffuse reflectance spectra of SiO_2-BP powders after the reduction of silver are shown in Fig. 5 after filtration and drying. The SPR absorption bands of SiO_2-BP powder (Fig. 5 curve 1) and solution with SiO_2-BP film (Fig. 2a) are similar, suggesting that the silver nanoparticles are located on the SiO_2-BP powders. The importance of Ludox in the solution to stabilize the silver nanoparticles is demonstrated in Fig. 5 by comparing curve 1 (Ludox) with curve 2 (no Ludox). The red shift and broadening of the reflectance spectrum in curve 2 is due to aggregation and growth of the silver nanoparticles in the absence of Ludox; SiO_2-BP powder was unable to stabilize the nanoparticles, and the powder was only a method for introduction (and removal) of BP into (and out of) the solution. This suggests that in the absence of Ludox, strong interactions between neighboring silver nanoparticles occurred. Thus, with the SiO_2-BP powders the silver nanoparticles attached to the silica surface, while no nanoparticle attachment was observed on the SiO_2-BP film. This was probably due to the small pore size of the silica for embedding silver nanoparticles, a smaller available surface, and a smaller charge density compared with SiO_2-BP powder.

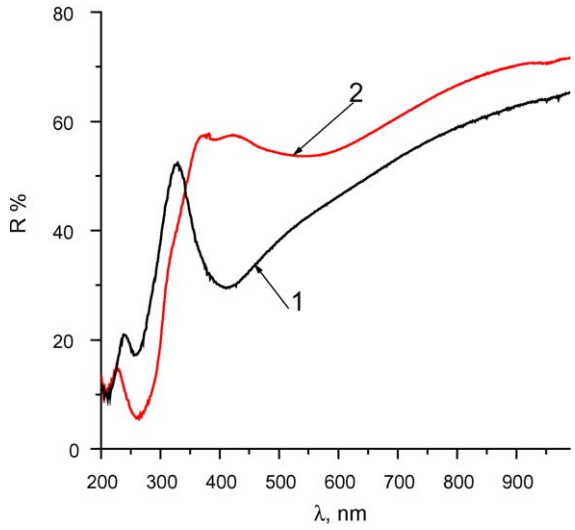

Fig. 5. Diffuse reflectance spectra of SiO_2-BP powder after photoreduction of silver in solution: with Ludox (1) and without Ludox (2). Ludox acts as a stabilizing material.

3.7. Photoinduced formation of SiO_2-Ag films

Silica films doped with Ag^+ were synthesized via the sol–gel route (as described in Section 2.6) in order to produce a material with a uniform distribution of Ag nanoparticles. Irradiation of the SiO_2-Ag film in an aqueous solution of BP, SDS, and IPA resulted in the photoreduction of the embedded silver ions and the appearance of the typical surface plasmon resonance absorption band centered at 408 nm (Fig. 6a). The XRD pattern of the SiO_2-Ag film consists of Ag (1 1 1), Ag (2 0 0), Ag (2 2 0), and Ag (3 1 1) diffraction peaks (supplementary Fig. S.4). The silver nanoparticle diameter calculated by the Scherrer equation [39] is about 7 nm.

An SEM image of silver nanoparticles embedded in the silica film after irradiation is shown in Fig. 6b, confirming the presence of silver nanoparticles on the surface and in the interior of the silica film. Particle size is observed to be 5–10 nm, which is in agreement with the value obtained from XRD. The nanoparticles are embedded in the silica matrix, thus making it difficult to obtain a clear picture of them. The blurring of the sample is due to the silica-insulating layer between the particles and the electron beam.

To determine the adhesion of silver nanoparticles to the silica surface after the photoreduction of the SiO_2-Ag film in BP solution, the surface was repeatedly washed with aqueous solution. Absorption measurements were taken of the aqueous solution after washing and no surface plasmon resonance of silver nanoparticles was detected; therefore adhesion is suggested to be good.

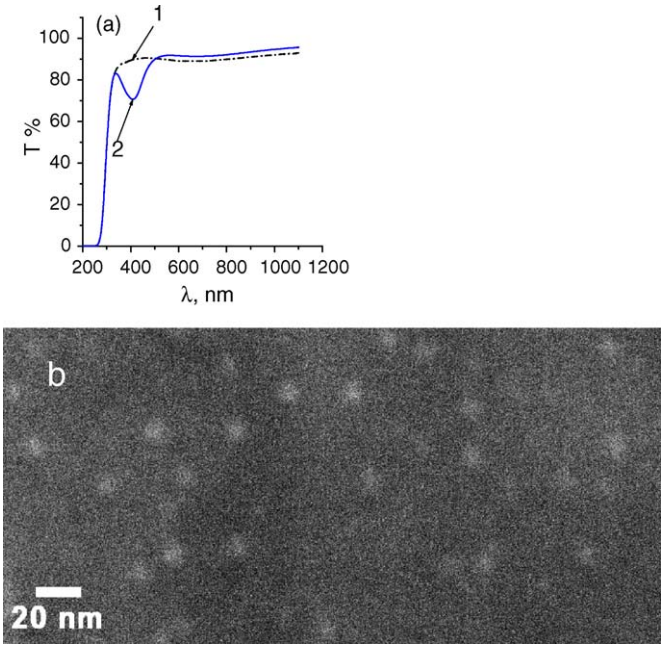

Fig. 6. (a) Transmittance spectra of SiO_2-Ag films before (1) and after irradiation (2); (b) SEM image reveals silver particles formed embedded in the porous silica film. The light spots are the silver nanoparticles.

This technique offers the possibility of producing silica films and powders with embedded silver particles, which allow the fabrication of highly conductive materials and firmly anchored nanoparticle catalysts, thereby suppressing loss of catalytic activity due to nanoparticle aggregation.

3.8. pH kinetic studies of SiO_2-BP powders

To further elucidate the mechanism, the pH dependence of the reaction was studied (Section 2.11). The absorption of silver nanoparticles is plotted versus the irradiation time in Fig. 7 for various pH values. The constant of the quasi-zero order reaction rate k_0 can be expressed as $k_0 = k/\alpha l$, where k is the slope of the linear plot. The calculated k_0 values for different pH value's presented in the inset of Fig. 7 were obtained for linear portions of the absorption in the first 45 min. The results show that the reduction proceeds slower in an acidic environment than in a neutral or basic one (Fig. 7) and can be explained by two reactions. As previously reported, the BP triplet can be quenched by a proton (in acidic conditions) [40]. However, the acid–base equilibrium of IPA and BP ketyl-radicals [26,41] is also considered. The anion-radicals of BP and IPA, formed during protolytic dissociation, are more reactive reducing species than ketyl-radicals and could contribute to the Ag^+ photoreduction in basic conditions, as this is the dominant species at higher pH values [42]. In acidic solutions, the formation of a BP anion-radical is suppressed, as shown in [41]:

$$(C_6H_5)_2C^{\bullet}O^- + H+ \leftrightarrow (C_6H_5)_2C^{\bullet}OH$$

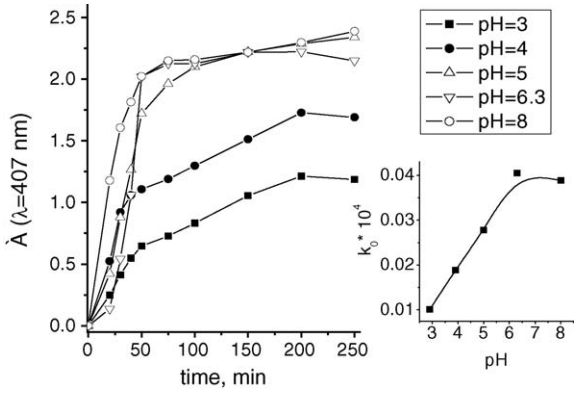

Fig. 7. pH dependence of the kinetics of Ag nanoparticle formation (determined from the absorption maximum of the silver nanoparticles as a function of irradiation time). Inset: pH dependence of the rate constant.

3.9. Proposed silver ion photoreduction mechanism

In accordance with previous publications [2,26,43] and based on the results discussed above, the following reaction mechanism is proposed:

(1) Photoexcitation of the triplet state of adsorbed benzophenone:

$$(C_6H_5)_2C{=}O \xrightarrow{h\upsilon} (C_6H_5)_2C{=}O^*$$

(2) Hydrogen atom abstraction by benzophenone triplet from isopropanol:

$$(C_6H_5)_2C{=}O^* + (CH_3)_2CHOH \rightarrow (C_6H_5)_2C^{\bullet}OH + (CH_3)_2C^{\bullet}OH$$

$$(C_6H_5)_2C{=}O + (CH_3)_2C^{\bullet}OH \rightarrow (C_6H_5)_2C^{\bullet}OH + (CH_3)_2C{=}O$$

(3) Quenching of BP triplet by silver ions:

$$(C_6H_5)_2C{=}O^* \xrightarrow{Ag^+} (C_6H_5)_2C{=}O$$

(4) Protolytic dissociation of ketyl-radicals [26,44]:

$$R_2C^{\bullet}OH \rightarrow R_2C^{\bullet}O^- + H^+$$

The electrochemical potential from solution is presented in an attempt to quantify the reduction by various species on the silica surface. The ketyl-radicals have strong reducing properties. The electrochemical potentials of $(CH_3)_2C^{\bullet}OH$ and BP ketyl-radicals, $(C_6H_5)_2C^{\bullet}OH$, are equal to −1.39 and −1.1 V, respectively while the Ag^+/Ag potential is −1.8 V [26]. Therefore, unless a large change in these potentials takes place on the silica surface, these ketyl-radicals are not very effective in reducing Ag^+. The radical anion of BP possesses a greater negative electrochemical potential in comparison with the ketyl ones, namely −1.81 V for $(C_6H_5)_2C^{\bullet}O^-$ and −2.1 V for $(CH_3)_2C^{\bullet}O^-$ [45]. Due

to the electrochemical potentials and pH results, we propose that the radical anion is responsible for initial silver ion reduction. We propose that both ketyl-radicals [46] and anion-radicals are involved in the next step:

(5) Reduction of silver ions:

$$R_2C^{\bullet}OH + Ag^+ \rightarrow R_2C{=}O + Ag^0 + H^+$$

$$R_2C^{\bullet}O^- + Ag^+ \rightarrow R_2C{=}O + Ag^0, \quad R = CH_3, C_6H_5$$

(6) Silver nanoparticle formation:

$$nAg \rightarrow (Ag)_n$$

(7) Silver nanoparticle peptization by benzophenone ketyl-radical analogous with Yonezawa et al. [43]:

$$(C_6H_5)_2C^{\bullet}OH + (Ag^0)_n \rightarrow (C_6H_5)_2CO + (Ag^0)_n{}^- + H^+$$

(8) Silver nanoparticle growth:

$$(Ag^0)_n{}^{m-} + Ag^+ \rightarrow (Ag^0)_{n+1}{}^{(m-1)-}$$

During the first stage of the photoreduction process, only a small number of silver particles are formed. Then a secondary reduction occurs (8) in which silver ions are reduced on the surface of the initial nanoparticles. This process occurs in two steps, electron transfer from BP-ketyl-radicals to the silver nanoparticle (reaction 5) and further reduction of silver ions by the electrons stored on the nanoparticle's surface (reaction 8) [26,44].

4. Conclusion

Porous sol–gel produced silica films and powders modified with adsorbed benzophenone molecules were found to be effective in the photoreductive formation of silver nanoparticles. SiO_2 film and powder was used as a convenient carrier for the photoactive compound BP, which is not soluble in water. Immobilization of BP on the SiO_2 surfaces controlled the presence of BP in solution and facilitated its removal. The formation of Ag nanoparticles within a thin silica film (SiO_2-Ag) was also achieved by introducing Ag^+ ions into the SiO_2 matrix during the sol–gel preparation and subsequent irradiation in a BP–IPA medium.

Emission spectra of adsorbed BP on the SiO_2 surface were observed. The pH dependence was measured to improve the understanding of the reaction mechanism and is presented herein. These measurements add to the understanding of a complex reduction by benzophenone of silver in aqueous solutions and to the complex field of heterogeneous catalysis. These structures can be used for diverse purposes such as supported catalysis of metal clusters, removal of metal ions from solution, and increased conductivity of silica films.

Appendix A. Supplementary data

Supplementary data associated with this article can be found, in the online version, at doi:10.1016/j.jphotochem.2005.12.024.

References

[1] S. Kapoor, D.K. Palit, T. Mukherjee, Chem. Phys. Lett. 355 (2002) 383–387.
[2] N. Kometani, H. Doi, K. Asami, Y. Yonezawa, Phys. Chem. Chem. Phys. 4 (2002) 5142–5147.
[3] T. Sato, N. Maeda, H. Ohkoshi, Y. Yonezawa, Bull. Chem. Soc. Jpn. 67 (1994) 3165–3171.
[4] P. Yankov, Z. Nickolov, V. Zhelyaskov, J. Photochem. Photobiol. 47 (1988) 155–165.
[5] C.F. Bohren, D.R. Huffman, Absorption and Scattering of Light by Small Particles, Wiley, New York, 1983.
[6] P. Hildebrandt, M. Stockburger, J. Phys. Chem. 88 (1984) 5935–5944.
[7] E. Janata, A. Henglein, B.G. Ershov, J. Phys. Chem. 98 (1994) 10888–10890.
[8] P.V. Kamat, M. Flumiani, A. Dawson, Colloid Surf. A 202 (2002) 269.
[9] D. Lawless, S. Kapoor, P. Kennepohl, D. Meisel, N. Serpone, J. Phys. Chem. 98 (1994) 9619–9625.
[10] Z.S. Pillai, P.V. Kamat, J. Phys. Chem. B 108 (2004) 945–951.
[11] T. Ung, L.M. Liz-Marzan, P. Mulvaney, Langmuir 14 (1998) 3740–3748.
[12] A. Henglein, Ber. Bunsen-Ges. Phys. Chem. 84 (1980) 253–259.
[13] A. Eremenko, N. Smirnova, L. Spanhel, O. Rusina, L. Linnik, B. Eremenko, K. Rechthaler, J. Mol. Struct. 553 (2000) 1–7.
[14] N. Smirnova, A. Eremenko, O. Rusina, W. Hopp, L. Spanhel, J. Sol–Gel Sci. Tech. 21 (2001) 109–113.
[15] T. Yamada, K. Asai, A. Endo, H.S. Zhou, I. Honma, J. Mater. Sci. Lett. 19 (2000) 2167–2169.
[16] S. Eustis, G. Krylova, A. Eremenko, N. Smirnova, A.W. Schill, M.A. El-Sayed, Photochem. Photobio. Sci. 4 (2005) 154–159.
[17] C.G. Hatchard, C.A. Parker, Proc. Roy. Soc. Lond. Ser. A 518 (1956) 518–537.
[18] L. Viaene, D. Meerschaut, M. Van Der Auweraer, F.C. De Schryver, F. Wilkinson, Res. Chem. Intermed. 21 (N7) (1995) 711–723.
[19] E.H. Gilmore, G.E. Gibson, D.S. McClure, J. Chem. Phys. 20 (1953) 829–834.
[20] S.P. McGlynn, T. Azumi, M. Kinoshita, Molecular Spectroscopy of the Triplet State, Prentice-Hall, New York, 1969.
[21] B. Shah, D.C. Neckers, The photochemistry of benzophenone, Spectrum 16 (2003) 18–21.
[22] A. Demeter, T. Berces, J. Photochem. Photobiol. A 46 (1989) 27–40.
[23] N.J. Turro, M.B. Zimmt, I.R. Gould, J. Am. Chem. Soc. 107 (1985) 5826–5827.
[24] J.K. Thomas, Photochem. Photobio. Sci. 3 (2004) 483–488.
[25] N. Turro, Modern Molecular Photochemistry, The Benjamin–Cummings Publishing Co., CA, 1978.
[26] A. Henglein, Chem. Mater. 10 (1998) 444–450.
[27] H. Nishiguchi, S. Okamoto, M. Nishimura, H. Yamashita, M. Anpo, Res. Chem. Intermed. 24 (1998) 849–858.
[28] S. Okamoto, H. Nishiguchi, M. Anpo, Chem. Lett. (1992) 1009.
[29] A. Eremenko, N. Smirnova, Funct. Mater. 3 (1996) 511–517.
[30] A. Henglein, J. Phys. Chem. 97 (1993) 5457–5471.
[31] R.H. Doremusm, J. Chem. Phys. 42 (1965) 414–417.
[32] A. Henglein, P. Mulvaney, Faraday Discuss. 92 (1991) 31–44.
[33] J.R. Rabek, Experimental Methods in Photochemistry and Photophysics, Willey, New York, 1982.
[34] A. Henglein, J. Phys. Chem. 83 (1979) 2209–2216.
[35] H. Hada, Y. Yonezawa, A. Yoshida, A. Kurakake, J. Phys. Chem. 80 (1976) 2728–2731.
[36] U. Kreibig, M. Vollmer, Optical Properties of Metal Clusters, Springer, Berlin, 1995.
[37] L.L. Zhao, K.L. Kelly, G.C. Schatz, J. Phys. Chem. B 107 (2003) 7343–7350.

[38] T.B. Boitsova, V.V. Gorbunova, E.I. Volkova, Russ. J. Gen. Chem. 72 (2002) 642–656.
[39] B. Hincapie, L. Garces, Q. Zhang, A. Sacco, L.S. Suib, Micropor. Mesopor. Mater. 67 (2004) 19–22.
[40] M.B. Ledger, G. Porter, J. Chem. Soc. Faraday Trans. 57 (1961) 539–553.
[41] J.L. Marignier, B. Hickel, J. Phys. Chem. 88 (1984) 5375–5379.
[42] G. Porter, F. Wilkinson, Trans. Faraday Soc. 57 (1961) 1686–1691.
[43] Y. Yonezawa, T. Sato, S. Kuroda, J. Chem. Soc. Faraday Trans. 87 (1991) 1905–1910.
[44] S. Kundu, M. Mandal, S.K. Ghosh, T. Pal, J. Colloid Interf. Sci. 272 (2004) 134–144.
[45] A. Shwarz, R.W. Dodson, J. Phys. Chem. 93 (1989) 409–414.
[46] A.S. Korchev, M.J. Bozack, B.L. Slaten, G. Mills, J. Am. Chem. Soc. 126 (2004) 10–11.